NASA CONTRACTOR REPORT

NASA CR-285

NASA CR-2

ANALYSIS OF THE VISCO SEAL

PART I - THE CONCENTRIC LAMINAR CASE

by William K. Stair

Prepared under Grant No. NsG-587 *by*
UNIVERSITY OF TENNESSEE
Knoxville, Tenn.

for

NATIONAL AERONAUTICS AND SPACE ADMINISTRATION • WASHINGTON, D. C. • AUGUST 1965

ANALYSIS OF THE VISCO SEAL

PART I – THE CONCENTRIC LAMINAR CASE

By William K. Stair

Prepared under Grant No. NsG-587 by
UNIVERSITY OF TENNESSEE
Knoxville, Tenn.

for

NATIONAL AERONAUTICS AND SPACE ADMINISTRATION

For sale by the Clearinghouse for Federal Scientific and Technical Information
Springfield, Virginia 22151 – Price $2.00

ABSTRACT

This report presents a theoretical analysis of the visco-type shaft seal when operating concentrically in laminar flow. The analysis, which is patterned after the work of Boon and Tal, shows the development of the sealing coefficient and dissipation function. These two parameters have been computed for the range of seal geometries most likely to be encountered in practice and are presented in tabular form.

TABLE OF CONTENTS

I. INTRODUCTION

The visco seal, screw seal, viscosity pump, spiral groove seal or bearing are some of the various names given the device whose working principle is based on the head developed in a viscous fluid, enclosed in a thin annulus or slit, by means of grooves on a rotating shaft or plate. While the basic concept of the visco seal was formulated many years ago, only recently has the device been seriously considered as a sealing element in practical engineering systems. Recent studies of the visco seal, most of which have been made abroad, have been prompted by the need for reliable, long life, low leakage seals in critical engineering systems having demanding sealing specifications. Such systems are encountered in the nuclear power field and in the space programs.

A series of studies of various sealing concepts has been completed by personnel of the Mechanical and Aerospace Engineering Department at the University of Tennessee (1, 2, 3, 4). These studies indicate that of the various sealing concepts which may be considered for critical applications, the visco seal seems to hold the most promise of successful application. A similar conclusion has also resulted from other "state of the art studies" (5).

Although the contact type seal, the mechanical face seal for example, is widely used in normal engineering applications, the basic sealing mechanism is not well understood. Further, long experience points to a finite life. Considerable disagreement exists as to the most appropriate method of analysis and design (4).

The contactless seal has the advantage of long life and a history of reliable service. While many of the contactless seals are characterized by large leakage rates, especially when used in compact designs, the visco seal has the additional advantage of low leakage rates. Further, the visco seal can be designed to function automatically as a shut down seal when the shaft is not rotating. From a critical review (6) of all known published studies of the visco seal, the work of Boon and Tal (7) appears to be the most comprehensive and detailed analysis available on the subject.

The current program at the University of Tennessee, which is being conducted under auspices of the NASA, embraces both laminar and turbulent visco seal operation under concentric and eccentric conditions. While the study of Boon and Tal considers only the laminar concentric case, this work was selected as the basis for initial experimental studies under the present program. The analysis presented in this report is patterned after the work of Boon and Tal and presents the values of the sealing coefficient and the dissipation function for a wide range of geometries in a form which can be readily used by the seal designer.

II. THEORY

The Sealing Coefficient

Consider a screw formed on a shaft located concentrically within a cylindrical housing with a radial clearance c. The annular space is filled with a fluid and the shaft is moving relative to the housing with an angular velocity, ω. The arrangement of the screw and housing is shown in Figure 1. The threaded length of the screw is l, whereas the effective seal length is L. It has been observed that the performance of the visco seal or visco pump having a threaded housing and a plain shaft is essentially the same as for the arrangement shown in Figure 1. (8, 9).

Figure 2 shows a developed view of the visco seal geometry with two sets of coordinates. The (x, y) axes are along and normal to the direction of relative motion and the (ξ, η) axes are parallel and normal to the grooves. The (x, y) and (ξ, η) coordinate systems are related by:

$$\xi = x \cos\alpha + y \sin\alpha \tag{1}$$

$$\eta = y \cos\alpha - x \sin\alpha \tag{2}$$

For simplicity the plain surface is assumed to have a velocity $U = 1/2\ \omega D$. Assuming a Newtonian fluid having a negligible change in density, the equations of motion and continuity for laminar flow are:

$$\left.\begin{aligned} \rho \frac{Du}{Dt} &= F_\xi - \frac{\partial p}{\partial \xi} + \mu \nabla^2 u \\ \rho \frac{Dv}{Dt} &= F_\eta - \frac{\partial p}{\partial \eta} + \mu \nabla^2 v \\ \rho \frac{Dw}{Dt} &= F_z - \frac{\partial p}{\partial z} + \mu \nabla^2 w \end{aligned}\right\} \tag{3}$$

$$\frac{\partial u}{\partial \xi} + \frac{\partial v}{\partial \eta} + \frac{\partial w}{\partial z} = 0 \tag{4}$$

Assuming steady incompressible flow, noting that c/D is so small as to render w negligible with negligible pressure change in the Z direction, and neglecting body forces as being small in comparison with viscous forces, there remains from equation (3) the following gradients:

$$\frac{\partial^2 u}{\partial z^2} = \frac{1}{\mu} \frac{\partial p}{\partial \xi} \tag{5}$$

$$\frac{\partial^2 v}{\partial z^2} = \frac{1}{\mu} \frac{\partial p}{\partial \eta} \tag{6}$$

Integration of (5) and (6) gives:

$$u = \frac{1}{2\mu}\frac{\partial p}{\partial \xi} z^2 + C_1 z + C_2 \tag{7}$$

$$v = \frac{1}{2\mu}\frac{\partial p}{\partial \eta} z^2 + C_3 z + C_4 \tag{8}$$

The velocities in the region of the grooves and in the region of the lands or ridges may be determined by noting the following boundary conditions:

Along the lands	Across the lands
$u_r = U \cos \alpha$ at $Z = 0$	$v_r = -U \sin \alpha$ at $Z = 0$
$u_r = 0$ at $Z = h_r$	$v_r = 0$ at $Z = h_r$

Along the grooves	Across the grooves
$u_g = U \cos \alpha$ at $Z = 0$	$v_g = -U \sin \alpha$ at $Z = 0$
$u_g = 0$ at $Z = h_g$	$v_g = 0$ at $Z = h_g$

Using the above boundary conditions the following velocity components may be identified:

Along the lands

$$u_r = -\frac{1}{2\mu}\frac{\partial p}{\partial \xi}\left(z h_r - z^2\right) + U \cos \alpha \left(1 - \frac{z}{h_r}\right) \tag{9}$$

Along the grooves

$$u_g = -\frac{1}{2\mu}\frac{\partial p}{\partial \xi}\left(z h_g - z^2\right) + U \cos \alpha \left(1 - \frac{z}{h_g}\right) \tag{10}$$

Across the lands

$$U_r = -\frac{1}{2\mu}\left(\frac{\partial p}{\partial \eta}\right)_r (zh_r - z^2) - U \sin\alpha\left(1 - \frac{z}{h_r}\right) \tag{11}$$

Across the grooves

$$U_g = -\frac{1}{2\mu}\left(\frac{\partial p}{\partial \eta}\right)_g (zh_g - z^2) - U \sin\alpha\left(1 - \frac{z}{h_g}\right) \tag{12}$$

Noting that the axial velocity components are

$$u_y = u \sin\alpha \qquad \text{and} \tag{13}$$

$$v_y = v \cos\alpha, \tag{14}$$

the axial flow components $Q_{\xi r}$, $Q_{\xi g}$, $Q_{\eta r}$ and $Q_{\eta g}$, may be computed. The width of the flow path for the ξ land flow component is $(1 - \gamma)\pi D$ and the path width for the ξ groove flow is $\gamma\pi D$. The ratio of the groove width to the groove plus land width is defined as γ.

$$\gamma = \frac{b}{a+b} \qquad \text{See Figure 1} \tag{15}$$

The axial component of the ξ coordinate land flow is:

$$Q_{\xi r} = (1-\gamma)\pi D\int_0^{h_r} u_{ry}\,dz = (1-\gamma)\pi D\int_0^{h_r} u_r \sin\alpha\, dz \tag{16}$$

Substituting equation (9) and integrating,

$$Q_{\xi r} = (1-\gamma)\pi D\left[-\frac{h_r^3}{12\mu}\frac{\partial p}{\partial \xi}\sin\alpha + \frac{Uh_r}{2}\cos\alpha\,\sin\alpha\right] \tag{17}$$

In a similar manner

$$Q_{\xi g} = \gamma \pi D \left[-\frac{h_g^3}{12\mu} \frac{\partial p}{\partial \xi} \sin \alpha + \frac{U h_g}{2} \cos \alpha \sin \alpha \right] \tag{18}$$

$$Q_{nr} = \pi D \left[-\frac{h_r^3}{12\mu} \left(\frac{\partial p}{\partial n} \right)_r \cos \alpha - \frac{U h_r}{2} \sin \alpha \cos \alpha \right] \tag{19}$$

$$Q_{ng} = \pi D \left[-\frac{h_g^3}{12\mu} \left(\frac{\partial p}{\partial n} \right)_g \cos \alpha - \frac{U h_g}{2} \sin \alpha \cos \alpha \right] \tag{20}$$

The pressure gradients in equations (17) through (20) may be replaced by the more convenient axial gradients by noting that:

$$\frac{\partial p}{\partial \xi} = \frac{\partial p}{\partial y} \sin \alpha , \quad \text{and} \tag{21}$$

$$(1-\gamma)\left(\frac{\partial p}{\partial n} \right)_r + \gamma \left(\frac{\partial p}{\partial n} \right)_g = \frac{\partial p}{\partial y} \cos \alpha \tag{22}$$

Noting, from Figure 2, that

$$h_r = c, \tag{23}$$

$$h = h_g - h_r, \text{ and} \tag{24}$$

$$h_g = \beta c \text{ where} \tag{25}$$

$$\beta = \frac{h + c}{c}, \tag{26}$$

and substituting equation (21), equations (17) and (18) become:

$$Q_{\xi r} = -\frac{\pi D(1-\gamma)c^3}{12\mu}\frac{\partial p}{\partial y}\sin^2\alpha + \frac{\pi DU(1-\gamma)c}{2}\cos\alpha\sin\alpha, \qquad (27)$$

$$Q_{\xi g} = -\frac{\pi D\gamma\beta^3c^3}{12\mu}\frac{\partial p}{\partial y}\sin^2\alpha + \frac{\pi DU\gamma\beta c}{2}\cos\alpha\sin\alpha. \qquad (28)$$

The law of continuity requires that

$$Q_{\eta r} = Q_{\eta g}. \qquad (29)$$

Thus,

$$Q = Q_{\xi r} + Q_{\xi g} + Q_{\eta r} = Q_{\xi r} + Q_{\xi g} + Q_{\eta g}. \qquad (30)$$

Combining equations (19), (20), (22) and (30) it may be shown that

$$\left(\frac{\partial p}{\partial n}\right)_r = \frac{\beta^3}{B}\frac{\partial p}{\partial y}\cos\alpha + \frac{6\mu U\gamma(\beta-1)}{Bc^2}\sin\alpha \qquad (31)$$

$$\left(\frac{\partial p}{\partial n}\right)_g = \frac{1}{B}\frac{\partial p}{\partial y}\cos\alpha - \frac{6\mu U(1-\gamma)(\beta-1)}{Bc^2}\sin\alpha \qquad (32)$$

where:

$$B = \beta^3(1-\gamma) + \gamma \qquad (33)$$

Substituting equation (31) equation (19) becomes:

$$Q_{nr} = -\frac{\pi D\beta^3c^3}{12\mu B}\frac{\partial p}{\partial y}\cos^2\alpha - \frac{\pi DUc}{2}\left[\frac{\gamma(\beta-1)}{B} + 1\right]\sin\alpha\cos\alpha \qquad (34)$$

Substituting equation (32) equation (20) becomes:

$$Q_{\eta g} = -\frac{\pi D \beta^3 c^3}{12\mu B}\frac{\partial p}{\partial y}\cos^2\alpha - \frac{\pi D U c}{2}\left[\beta - \frac{\beta^3(1-\gamma)(\beta-1)}{B}\right]\sin\alpha\cos\alpha \tag{35}$$

$$\frac{\gamma(\beta-1)}{B} + 1 = \beta - \frac{\beta^3(1-\gamma)(\beta-1)}{B} \tag{36}$$

Thus, $Q_{\eta r} = Q_{\eta g}$ as required by equation (29).

Writing the sine and cosine functions as tangents, letting $t = \tan\alpha$, and substituting equations (27), (28) and (34) or (27), (28) and (35) into equation (30), the axial flow becomes:

$$Q = -C_5\frac{\pi D c^3}{12\mu}\frac{\partial p}{\partial y} + C_6\frac{\pi D U c}{2} \tag{37}$$

$$C_5 = \left[\frac{\beta^3(1+t^2) + t^2\gamma(1-\gamma)(\beta^3-1)^2}{B(1+t^2)}\right] \tag{38}$$

$$C_6 = \left[\frac{\gamma t(1-\gamma)(\beta^3-1)(\beta-1)}{B(1+t^2)}\right] \tag{39}$$

While the visco seal may, under certain conditions, be useful as a sealing device when a net axial flow exists, the most useful situation would be to have Q equal to zero. Substituting:

$\frac{\Delta p}{L}$ for $\frac{\partial p}{\partial y}$, setting $Q = 0$, and rearranging:

$$\frac{6\mu UL}{\Delta pc^2} = \frac{C_5}{C_6} \tag{40}$$

The dimensionless group on the left of equation (40) is defined as the sealing coefficient.

$$\Lambda = \frac{6\mu UL}{\Delta p\, c^2} = \frac{\beta^3(1+t^2)+\gamma t^2(1-\gamma)(\beta^3-1)^2}{\gamma t(1-\gamma)(\beta^3-1)(\beta-1)} \tag{41}$$

It is observed that Λ is a function of the seal geometry alone. Equation (41) has been programed for digital computation and the sealing coefficient has been computed for the following ranges of goemetry factors:

t for α of 5° to 20°

β from 2 to 19

γ from 0.1 to 0.8

The variation of Λ as a function of geometry is graphically shown in Figures 3 - 6.

Note that the term L included in the sealing coefficient refers, as shown in Figure 1, to the active seal length and not to the total threaded length of the screw.

The Dissipation Function

Assuming steady state, neglecting thermal conduction and extrusion energy, it may be shown that the time rate of energy dissipation in the fluid by viscous action per unit volume of flow is: (10, 11).

$$q''_{f\xi} = \mu\left(\frac{\partial u}{\partial z}\right)^2 \tag{42}$$

$$q''_{f\eta} = \mu\left(\frac{\partial v}{\partial z}\right)^2 \tag{43}$$

From equations (9) through (12)

$$q''_{f\xi r} = \mu\left[-\frac{1}{2\mu}\frac{\partial p}{\partial \xi}(h_r - 2z) - \frac{U\cos\alpha}{h_r}\right]^2 \tag{44}$$

$$q''_{f\xi g} = \mu\left[-\frac{1}{2\mu}\frac{\partial p}{\partial \xi}(h_g - 2z) - \frac{U\cos\alpha}{h_g}\right]^2 \tag{45}$$

$$q''_{f\eta r} = \mu\left[-\frac{1}{2\mu}\left(\frac{\partial p}{\partial \eta}\right)_r(h_r - 2z) + \frac{U\sin\alpha}{h_r}\right]^2 \tag{46}$$

$$q''_{f\eta g} = \mu\left[-\frac{1}{2\mu}\left(\frac{\partial p}{\partial \eta}\right)_g(h_g - 2z) + \frac{U\sin\alpha}{h_g}\right]^2 \tag{47}$$

The rate of energy dissipation per unit area may be expressed as:

$$q'_{fr} = \int_0^{h_r} q''_{fr}\,dz \tag{48}$$

$$q'_{fg} = \int_0^{h_g} q''_{fg}\,dz \tag{49}$$

Substituting equations (44) through (47)

$$q'_{\xi r} = \frac{h_r^3}{12\mu}\left(\frac{\partial p}{\partial \xi}\right)^2 + \frac{\mu U^2 \cos^2\alpha}{h_r} \tag{50}$$

$$q'_{\xi g} = \frac{h_g^3}{12\mu}\left(\frac{\partial p}{\partial \xi}\right)^2 + \frac{\mu U^2 \cos^2\alpha}{h_g} \tag{51}$$

$$q'_{\eta r} = \frac{h_r^3}{12\mu}\left(\frac{\partial p}{\partial \eta}\right)_r^2 + \frac{\mu U^2 \sin^2\alpha}{h_r} \tag{52}$$

$$q'_{\eta g} = \frac{h_g^3}{12\mu}\left(\frac{\partial p}{\partial \eta}\right)_g^2 + \frac{\mu U^2 \sin^2\alpha}{h_g} \tag{53}$$

The components of power loss may be evaluated as the product of q' and the associated area. The land area and groove area are respectively:

$$A_r = (1 - \gamma)\pi DL \tag{54}$$

$$A_g = \gamma \pi DL \tag{55}$$

Thus the components of power loss associated with the flow components are:

$$q_{\xi r} = (1-\gamma)\pi DL\, q'_{\xi r} \tag{56}$$

$$q_{\xi g} = \gamma \pi DL\, q'_{\xi g} \tag{57}$$

$$q_{\eta r} = (1-\gamma)\pi DL\, q'_{\eta r} \tag{58}$$

$$q_{\eta g} = \gamma \pi DL\, q'_{\eta g} \tag{59}$$

Substituting c and βc for h_r and h_g respectively, and noting that the total power loss may be expressed as:

$$q = q_{\xi r} + q_{\xi g} + q_{\eta r} + q_{\eta g}, \tag{60}$$

the total energy dissipation rate becomes:

$$q = \frac{\pi D L c^3}{12\mu}\left[(1-\gamma+\gamma\beta^3)\left(\frac{\partial p}{\partial \xi}\right)^2 + (1-\gamma)\left(\frac{\partial p}{\partial n}\right)_r^2 + \gamma\beta^3\left(\frac{\partial p}{\partial n}\right)_g^2\right]$$

$$+ \frac{\mu\pi D L U^2}{c}\left[1-\gamma+\frac{\gamma}{\beta}\right] \tag{61}$$

Replacing the pressure gradients of equation (61) with $\frac{\partial p}{\partial y}$ according to equations (21), (31) and (32), noting from equation (41) that

$$\frac{\partial p}{\partial y} = \frac{\Delta p}{L} = \frac{6\mu U}{\Lambda c^2} \quad , \tag{62}$$

and writing the sine and cosine functions as tangents, equation (61) becomes:

$$q = \frac{\mu\pi D L U^2}{c}\left[\left(1-\gamma+\frac{\gamma}{\beta}\right) + 3\left\{\frac{t^2\gamma(1-\gamma)(\beta-1)^2(1-\gamma+\gamma\beta^3)}{\beta^3(1+t^2)+t^2\gamma(1-\gamma)(\beta^3-1)^2}\right\}\right] \tag{63}$$

Equation (63) can be written as:

$$q = \Phi\,\frac{\pi\mu D L U^2}{c} \tag{64}$$

where Φ , the dissipation function, corresponding to the bracketed term of equation (63), is a function of the seal geometry.

$$\Phi = \phi' + \phi'' \tag{65}$$

$$\phi' = \left(1 - \gamma + \frac{\gamma}{\beta}\right) \tag{66}$$

$$\phi'' = 3\left\{\frac{t^2\gamma(1-\gamma)(\beta-1)^2(1-\gamma+\gamma\beta^3)}{\beta^3(1+t^2)+t^2\gamma(1-\gamma)(\beta^3-1)^2}\right\} \tag{67}$$

ϕ' represents the loss due to Couette flow and is independent of the angle α. ϕ'' represents the loss due to Poiseuille flow and depends upon α, β, and γ. Equations (65), (66) and (67) have been programed for digital computation.

The variation of Φ with geometry is graphically shown in Figures 3 - 7.

Simplified Analysis of Dissipation Function

It has been suggested that ϕ'', due to Poiseuille flow, was small in comparison to ϕ' and could be neglected (12). This approach assumes that the power loss can be written as:

$$\bar{q} = \mu U A \frac{\partial V_x}{\partial z} \tag{68}$$

The velocity gradients are taken as U/c over the land area A_r, and $U/\beta c$ over the groove area A_g.

Thus,

$$\bar{q} = \mu U \left[\frac{UA_r}{c} + \frac{UA_g}{\beta c}\right] \tag{69}$$

Noting that

$$A_g = \gamma \pi DL, \text{ and} \tag{70}$$

$$A_r = (1 - \gamma)\pi DL, \tag{71}$$

$$\bar{q} = \mu\frac{\pi DLU^2}{c}\left[1 - \gamma + \frac{\gamma}{\beta}\right] \tag{72}$$

or

$$\bar{q} = \phi' \mu\frac{\pi DLU^2}{c} \tag{73}$$

where

$$\phi' = 1 - \gamma + \frac{\gamma}{\beta} \tag{74}$$

as in equation (66).

The magnitude of the error caused by neglecting the Poiseuille contribution to the power loss is shown in Figure 7. The ratio ϕ''/ϕ' varies, for the region covered by Appendix B, from 0.045% to 71%. The smaller error occurs with visco seals having low values of α and γ while the more significant errors occur with larger values of α and γ. Since the larger values of α and γ are of most interest for practical seals, as may be seen from Figures 3 - 6, the simplified evaluation of the dissipation function may often be questionable.

III. DISCUSSION

Maximum Seal Head

From equation (41) it is noted that for selected values of μ, U, L and c, the maximum seal head corresponds to a minimum value for Λ. Taking partial derivatives of Λ with respect to γ, β and t, it is observed that:

$$\frac{\partial \Lambda}{\partial \gamma} = 0 \qquad \text{when} \qquad \gamma = 0.5$$

$$\frac{\partial \Lambda}{\partial \beta} = 0 \qquad \text{when} \qquad \beta = 3.6533$$

$$\frac{\partial \Lambda}{\partial t} = 0 \qquad \text{when} \qquad t = \left[\frac{\beta^3}{\beta^3 + \gamma(1-\gamma)(\beta^3-1)^2}\right]^{0.5}$$

$t = 0.28066$ ($\alpha = 15.6772°$). From equation (41) $\Lambda_{min} = 10.9677$ and Δp_{max} becomes:

$$\Delta p_{max} = 0.54706 \frac{\mu UL}{c^2}. \tag{75}$$

Minimum Power Loss

The values of α, β, and γ which produce the maximum sealing head do not, when substituted in equation (63), give the minimum dissipation function. This fact can be observed from Figures 3 to 5. It was shown by Boon and Tal that a limiting asymptotic value of the power loss was reached as $\gamma \to 1$ and $\beta \to \infty$ (7). Introducing equation (41) for Λ and rearranging, equation (64) becomes:

$$q = \Phi \frac{\pi \mu DLU^2}{c^2} = \frac{\Lambda \Phi}{6} \pi DUc\Delta p \tag{76}$$

For the limiting conditions $\Lambda\Phi = 6$ and

$$q_{min} = \pi DUc\Delta p \tag{77}$$

Using $\gamma = 0.5$, $\beta = 3.6533$, and $t = 0.28066$, the values corresponding to Δp_{max}, $\Phi = 0.74296$, and from equation (76) the power loss for the seal giving Δp_{max} is:

$$q = 1.3581\ \pi DUc\Delta p = 1.3581\ q_{min}. \tag{78}$$

The limiting condition can not be reached in practice; however, low values of Φ can be obtained by appropriate selection of the geometry factors α, β, and γ. For selected values of β, Boon and Tal computed the values of γ and t for which Φ became a minimum. These results are presented in Table 1.

TABLE 1

Geometry Factors for Minimum Power Loss for Selected Values of β. After Boon and Tal (7)

β	γ	t	α	Λ	Φ
2	0.59	0.56418	29°26'	11.43	1.0330
3	0.65	0.31798	17°38'	12.03	0.6764
4	0.70	0.21112	11°55'	12.42	0.5840
5	0.74	0.15530	8°50'	13.44	0.5120
6	0.77	0.12177	6°57'	14.70	0.4549
7	0.79	0.09928	5°40'	15.90	0.4122
8	0.81	0.08379	4°47'	17.31	0.3732
9	0.83	0.07267	4°9'	18.90	0.3381
10	0.84	0.06355	3°38'	20.13	0.3154

Design Generalizations

The seal designer may have only limited opportunity to utilize the designs of Table 1 due to limitations on screw generating machines, problems of differential thermal expansion, and tolerance requirements imposed by the fabrication techniques employed. Also, while a number of theoretical and empirical analyses of the visco seal have been made, truly precise experimental data suitable for correlation are not available (6, 13). The generation of such data is one of the major objectives of the current project. In the interim, however, some observations may be helpful to those wishing to use the present analysis in visco seal design.

Comparing Figures 3, 4, 5, which cover a normal range of α, it will be noted that the minimum value of the sealing coefficient obtainable for the various angles does not differ greatly. However, the seals with the lower helix angles allow for a wider variation in β for a given sealing coefficient. The lower helix angles also result in lower dissipation functions. As shown in Figure 6, this difference is most evident in the desirable β range of 2.5 to 7.0. While a γ value of 0.5 produces the lowest sealing coefficient at all helix angles, a substantial reduction in the dissipation function can be obtained with only a modest increase in the sealing coefficient by utilizing a larger value of γ .

The present analysis assumes laminar flow throughout the visco seal. Therefore, based on the Taylor instability criterion this analysis is strictly valid for operation below the critical Reynolds numbers which are:

$$R_{e_r} \equiv \frac{Uc\rho}{\mu} < 41.1 \sqrt{D/2c} \qquad (79)$$

$$R_{e_g} \equiv \frac{U\beta c\rho}{\mu} < 41.1\sqrt{D/2\beta c} \qquad (80)$$

The frictional losses occur largely in the land regions of the seal and the head developed is more dependent upon the groove flow. Thus, it would be expected that equation (79) should be used as the limiting condition when the dissipation function is being calculated and equation (80) is more appropriate when the sealing coefficient is being considered. The data presently available lend support to this generalization (12).

The present analysis also assumes that the plain and threaded surfaces are concentric. Such a situation is most unlikely in actual practice and no data are presently available which account for the expected eccentricity. A very limited analysis which attempts to include eccentricity has been made (12). This analysis starts with the assumption that the seal head developed varies inversely with eccentricity in a manner similar to the variation of axial flow through a plain annulus as a function of eccentricity. If both the shaft and sleeve are ungrooved, thus forming a simple annular flow system, then $\beta = 1$ and $\gamma = 0$ or 1. Under this condition equations (38) and (39) reduce to:

$C_5 = 1$ and $C_6 = 0$.

Thus equation (37) becomes

$$Q_{conc} = - \frac{\pi D c^3}{12\mu} \frac{\Delta p}{L} \qquad (81)$$

However, when Q is set equal to zero the pressure gradient becomes zero and the seal is incapable of developing a sealing head. Equation (81) represents the flow through a concentric annulus due to the imposed gradient. Also, for the plain annulus it may be shown that the flow under eccentric conditions due to the imposed gradient is expressed by

$$Q_{ecc} = - \frac{\pi D c^3}{12\mu} \frac{\Delta p}{L} \left[1 + 1.5\varepsilon^2\right] , \qquad (82)$$

where the factor $\left[1 + 1.5\varepsilon^2\right]$ varies from 1 to 2.5 as the eccentricity ratio varies from 0 to 1 (4). While the laminar flow through an eccentric annulus due to an imposed pressure gradient is correctly presented by equation (82), it appears premature to assume that the developed seal head will deteriorate in a similar manner. A series of experimental tests, including measurement of the seal eccentricity, is scheduled as a part of this program and should help to resolve this question. Nevertheless, all of the experimental data available reflect the fact that the actual head developed in the visco seal is less than that given by equation (41). Hughes (14) found that the head developed by the visco seal was about 12% below the calculated value, Asanuma (8) noted a deviation of about 22%, and Boon and Tal (7) suggest that a deviation of 20 to 50% be assumed in making use of the theoretical head calculation. The deviations referred to above were due to errors in temperature measurement, thermal expansion of the seal, vibration, and other experimental anamolies as well as the lack of concentricity.

NOMENCLATURE

A	area
B	geometry factor defined by equation (33)
C_1, C_2, C_3, C_4	constants of integration
C_5, C_6	coefficients defined by equations (38) and (39)
D	seal diameter
F	field force
L	active seal length
Q	sealant flow
U	surface velocity
a	axial land width
b	axial groove width
c	radial clearance
h	groove depth
h	film thickness (h_g, h_r)
l	length of seal thread
p	pressure
$q, \bar{q}$	power loss
q'	power loss per unit surface area
q''	power loss per unit flow volume
t	tangent of helix angle α
u,v,w	velocity components in ξ, η, z coordinates
x,y,z	coordinates
ξ, η	coordinates
α	helix angle

β	$\frac{h + c}{c}$
γ	$\frac{b}{a + b}$
Λ	sealing coefficient
Φ	dissipation function
ϕ'	Couette component in Φ
ϕ''	Poiseuille component in Φ
μ	absolute viscosity
ε	eccentricity ratio
ρ	density

Subscripts

r	refers to land
g	refers to groove
ξr	refers to ξ direction in region of land
ηr	refers to η direction in region of land
ξg	refers to ξ direction in region of groove
ηg	refers to η direction in region of groove
y	refers to axial component
conc	concentric
ecc	eccentric

REFERENCES CITED

1. Stair, W. K., "A Research Program on Dynamic Seals," Proceedings of the ORNL Conference on Rotating Machinery for GCR Application, April 2-4, 1962, USAEC Report TID-7631.

2. Carden, W. H., "The Mechanical Face Seal. A Survey of Literature on Sealing Theory," Report ME 5-62-TN3, The University of Tennessee, March 1962.

3. Arnold, F., W. K. Stair, "The Labyrinth Seal - Theory and Design," Report ME 5-62-1, The University of Tennessee, March 1962.

4. Stair, W. K., "Liquid-Buffered Bushing Shaft Seals for Large Gas Circulators," Int. Conf. on Fluid Sealing, Paper C5, April 17-19, 1961, BHRA, Harlow, Essex, England.

5. Aerojet-General Nucleonics," An Evaluation of the State-of-the-Art of High Speed Seals, Report AN-AGCR-759, December 1964.

6. Stair, W. K., "The Visco Seal - A Survey," Report ME 5-62-2, The University of Tennessee, March 1962.

7. Boon, E. F., S. E. Tal, "Hydrodynamische Dichtung fur rotierende Wellen," <u>Chemie-Ing-Technik</u>, Vol. 31, No. 3, January 31, 1959, pp. 202-12.

8. Asanuma, T., "Studies of the Sealing Action of Viscous Fluids," Int. Conf. on Fluid Sealing, Paper A3, April 17-19, 1961, BHRA, Harlow, Essex, England.

9. Frossel, W., "Hochtourige Schmierolpumpe," <u>Konstrucktion</u>, Vol. 12, No. 5, 1960, pp. 195-203.

10. Knudsen, J. G., D. L. Katz, Fluid Dynamics and Heat Transfer, McGraw-Hill Book Co., Inc., New York, 1958.

11. Pinkus, O., B. Sternlicht, Theory of Hydrodynamic Lubrication, McGraw-Hill Book Co., Inc., New York, 1961.

12. McGrew, J. M., J. D. McHugh, "Analysis and Test of the Screw Seal in Laminar and Turbulent Operation," The General Electric Advanced Technology Laboratories, Report No. 63GLG6, May 3, 1963.

13. Stair, W. K., "Theoretical and Experimental Studies of Visco-Type Shaft Seals," Mechanical and Aerospace Engineering Research Report ME-64-587-1, October 23, 1964. A Semi-annual progress report on NASA Grant NsG-587.

14. Hughes, D. P., "Shaft Seal for High Gas Pressures," Int. Conf. on Fluid Sealing, Paper C1, April 17-19, 1961, BHRA, Harlow, Essex, England.

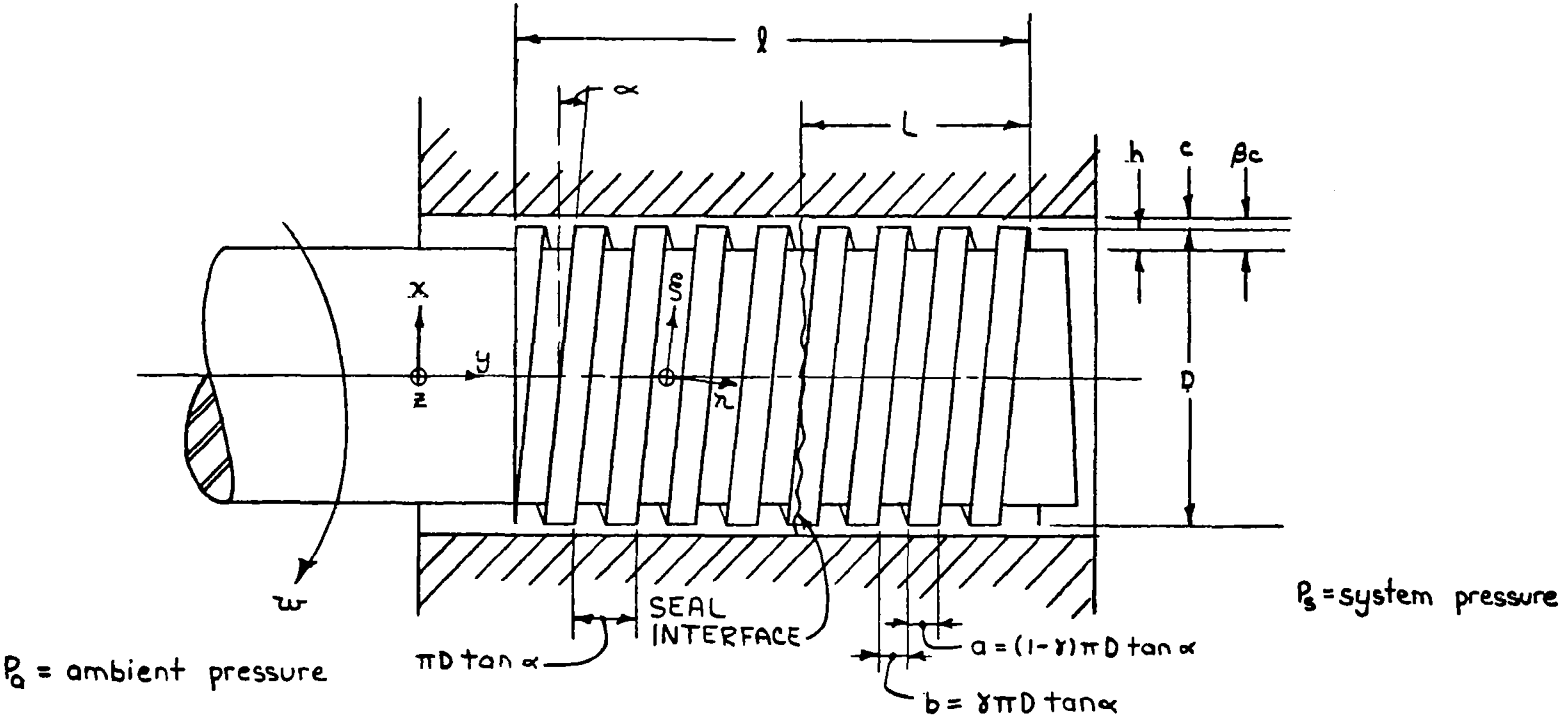

FIG. 1 - BASIC ELEMENTS OF A VISCO SEAL

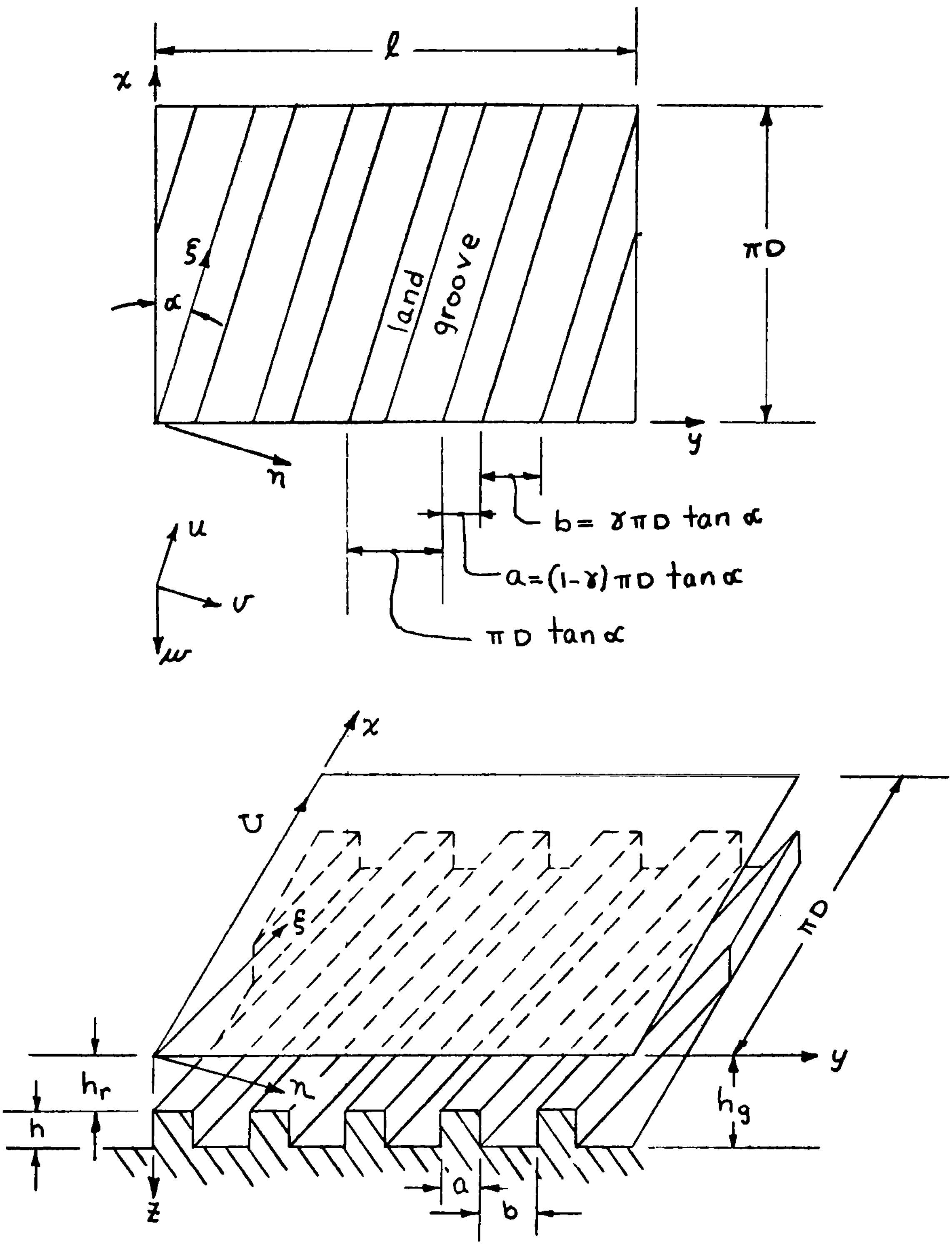

FIG. 2 - VISCO SEAL GEOMETRY

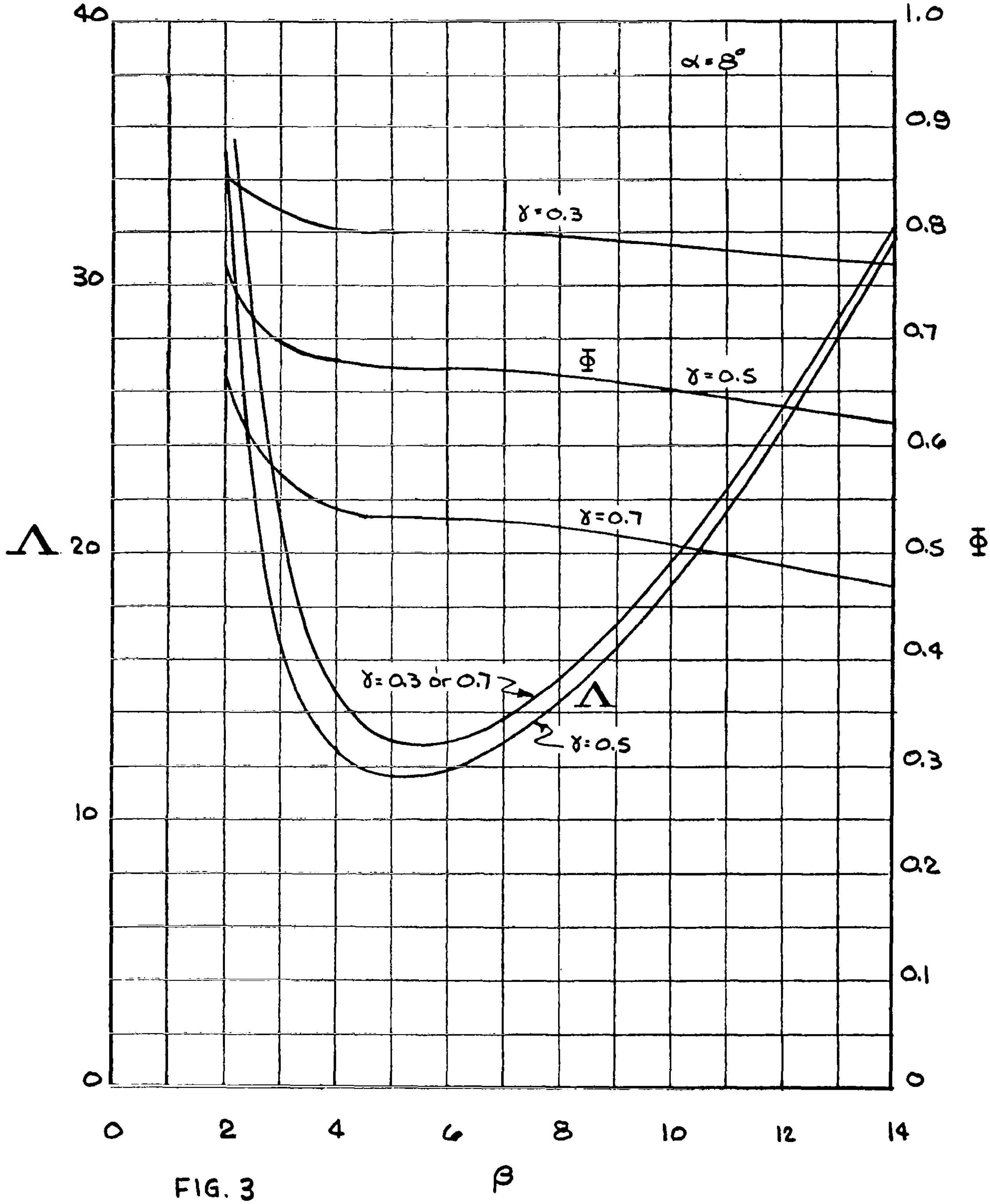

40
30
20
10
0
1.0
0.9
0.8
0.7
0.6
0.5
0.4
0.3
0.2
0.1
0
α = 8°
γ = 0.3
Φ
γ = 0.5
γ = 0.7
γ = 0.3 or 0.7
Λ
γ = 0.5
Λ
Φ
0
2
4
6
8
10
12
14
β

FIG. 3

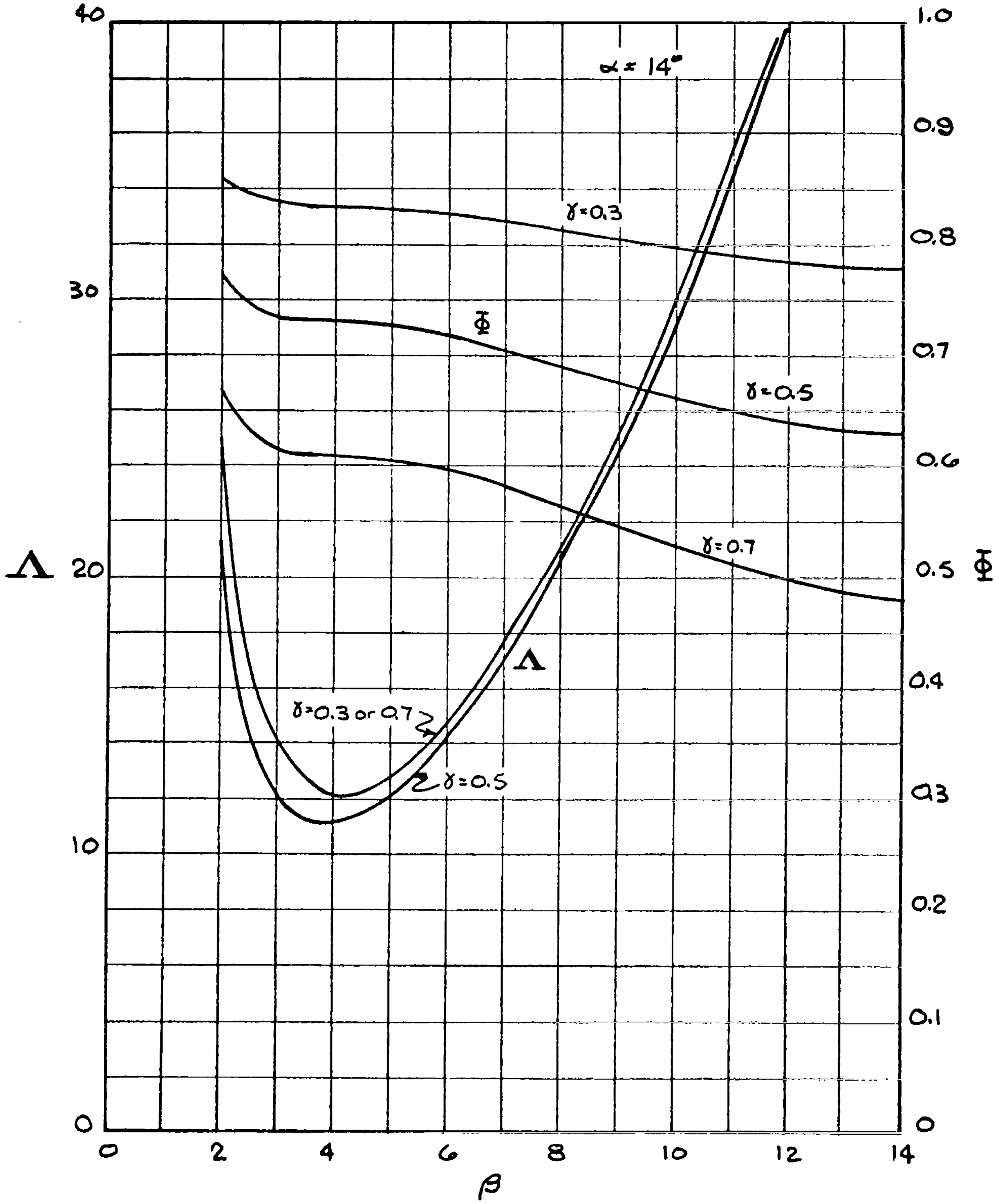

α = 14°
γ=0.3
Φ
γ=0.5
γ=0.7
Λ
γ=0.3 or 0.7
γ=0.5
Λ
Φ
β
40
30
20
10
0
1.0
0.9
0.8
0.7
0.6
0.5
0.4
0.3
0.2
0.1
0
0
2
4
6
8
10
12
14

FIG. 4

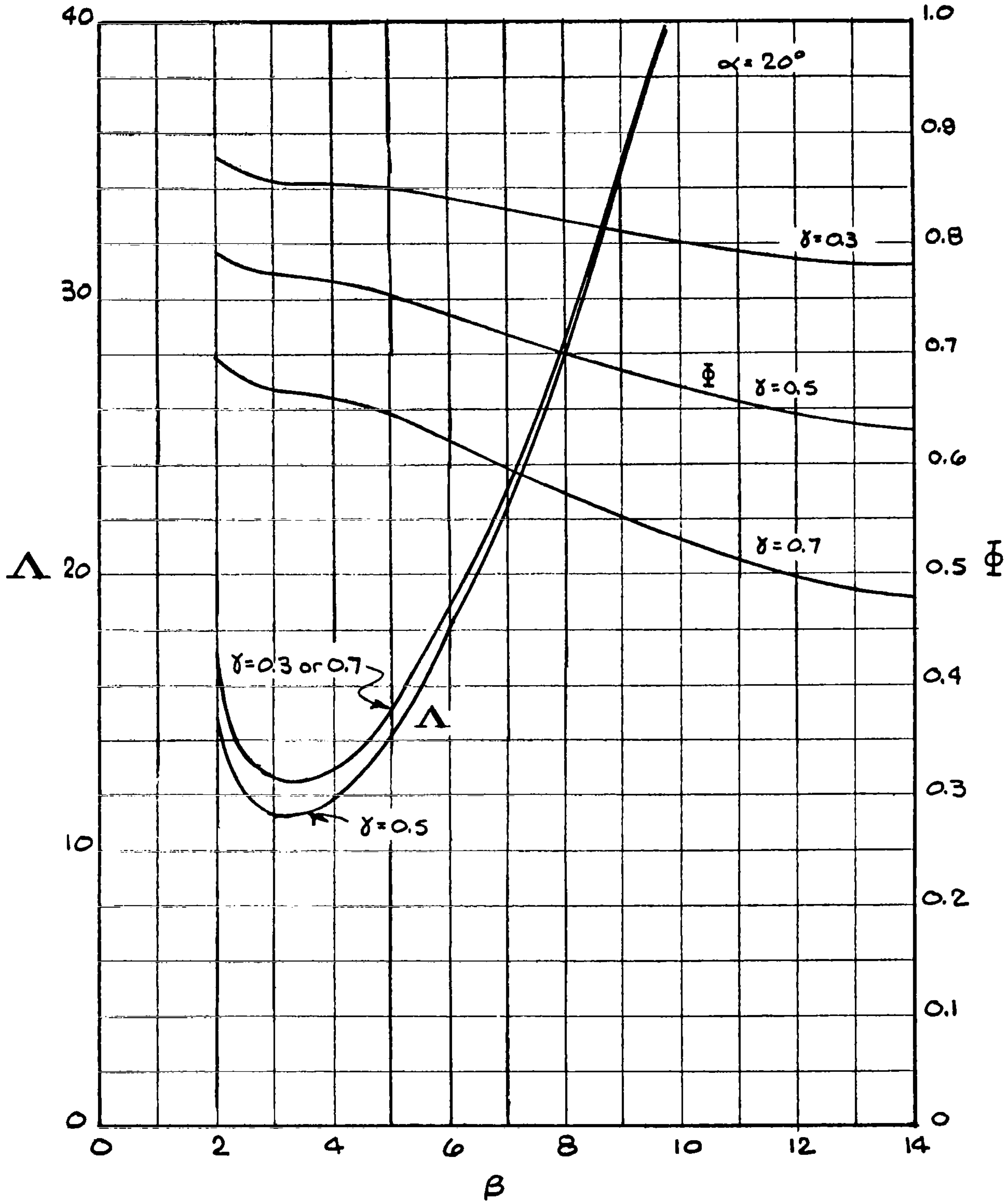

40
30
20
10
0
Λ
1.0
0.9
0.8
0.7
0.6
0.5
0.4
0.3
0.2
0.1
0
Φ
0
2
4
6
8
10
12
14
β
α = 20°
γ = 0.3
γ = 0.5
γ = 0.7
γ = 0.3 or 0.7
γ = 0.5
Λ
Φ

FIG. 5

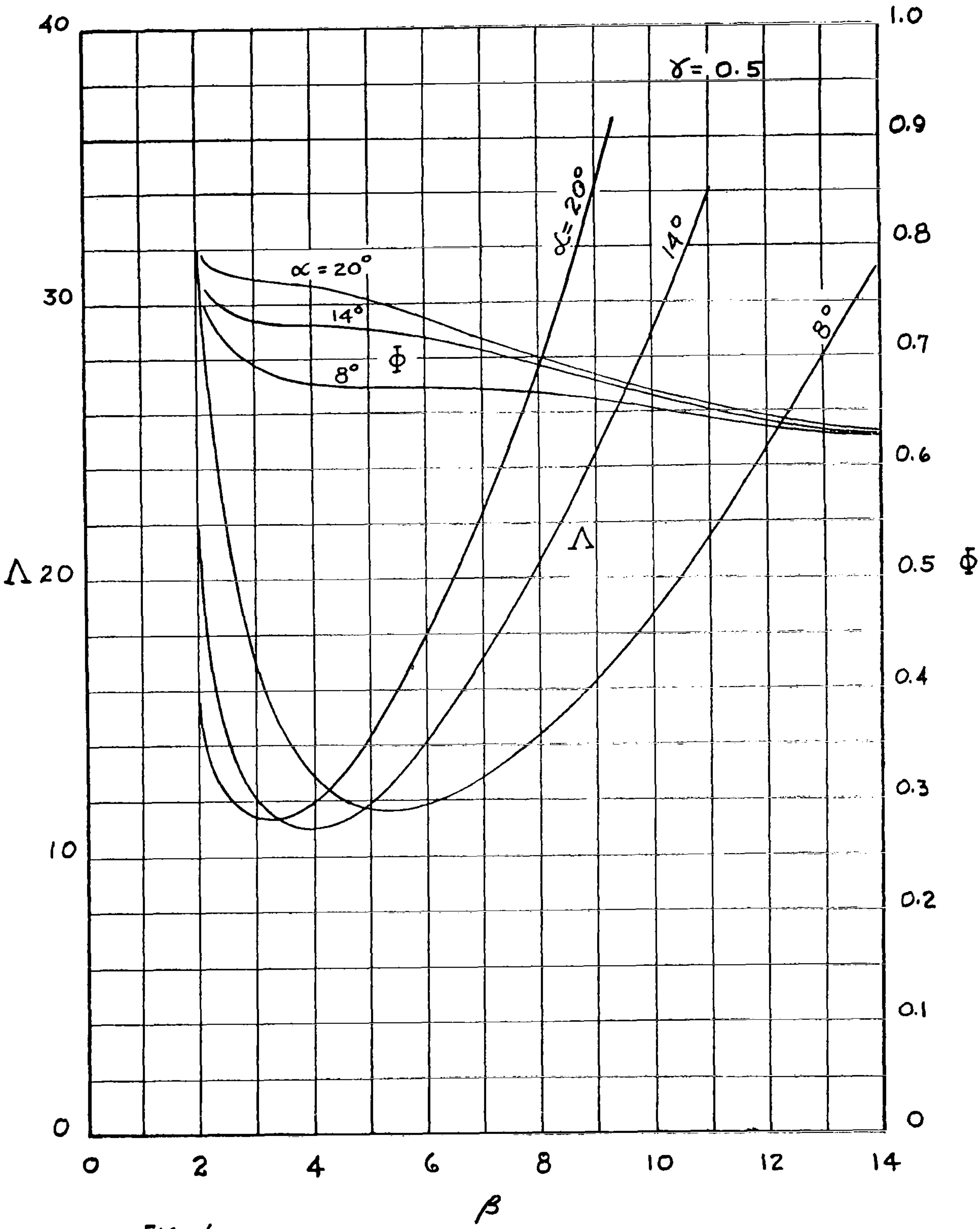
40
30
Λ 20
10
0
1.0
0.9
0.8
0.7
0.6
0.5 Φ
0.4
0.3
0.2
0.1
0
0
2
4
6
8
10
12
14
β
γ = 0.5
α = 20°
14°
8°
Φ
α = 20°
14°
8°
Λ

FIG. 6

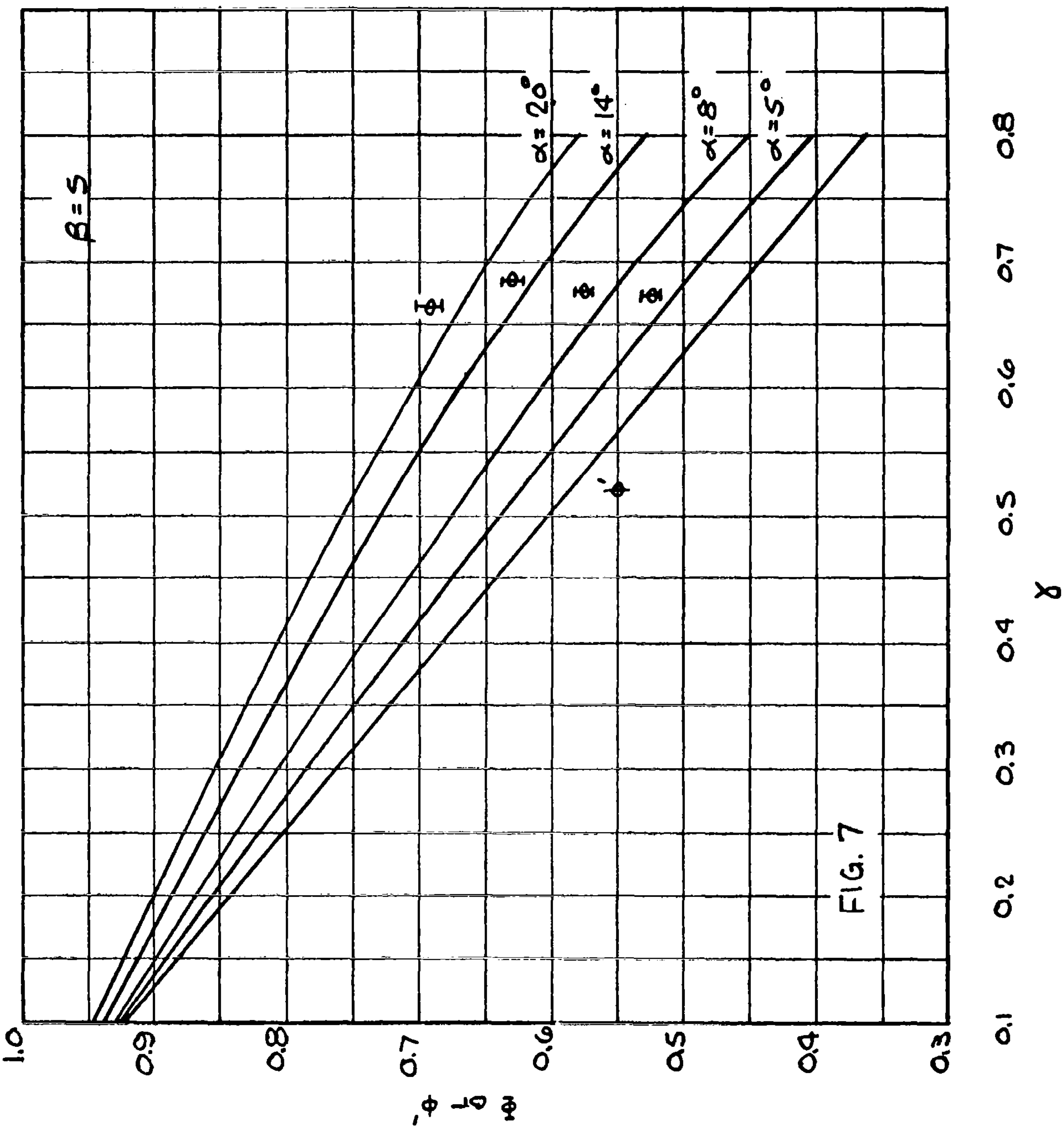

FIG. 7